

# Reduced Quasi-Dimensional Combustion Model of the Direct Injection Diesel Engine for Performance and Emissions Predictions

**Dohoy Jung\***

*Department of Mechanical Engineering, The University of Michigan,  
Ann Arbor, MI 48109-2121, USA*

**Dennis N. Assanis**

*Department of Mechanical Engineering, The University of Michigan,  
Ann Arbor, MI 48109-2121, USA*

A new concept of reduced quasi-dimensional combustion model for a direct injection diesel engine is developed based on the previously developed quasi-dimensional multi-zone model to improve the computational efficiency. In the reduced model, spray penetration and air entrainment are calculated for a number of zones within the spray while three zones with aggregated spray zone concept are used for the calculation of spray combustion and emission formation processes. It is also assumed that liquid phase fuel appears only near the nozzle exit during the breakup period and that spray vaporization is immediate in order to reduce the computational time. Validation of the reduced model with experimental data demonstrated that the new model can predict engine performance and NO and soot emissions reasonably well compared to the original model. With the new concept of reduced model, computational efficiency is significantly improved as much as 200 times compared to the original model.

**Key Words :** Diesel, Emissions, Quasi-dimensional, Multi-zone, Combustion model, Simulation

## Nomenclature

$A$  : Constant shown in Eqs. (19) and (20)  
 $B$  : Constant shown in Eqs. (6) and (7)  
 $C_D$  : Discharge coefficient  
 $d$  : Diameter  
 $E$  : Activation energy  
 $H$  : Hydrogen  
 $k$  : Forward rate constant  
 $m$  : Mass  
 $N$  : Nitrogen  
 $NO$  : Nitric Oxide  
 $O$  : Oxygen

$OH$  : Hydroxyl  
 $P$  : Pressure  
 $R$  : Chemical reaction rate  
 $\bar{R}$  : Universal gas constant  
 $RR$  : Reaction rate  
 $S$  : Spray penetration  
 $T$  : Temperature  
 $t$  : Time  
 $u$  : Velocity  
 $V$  : Volume  
 $x$  : Mass fraction

## Greek symbols

$\Delta P$  : Pressure difference  
 $\rho$  : Density  
 $\tau$  : Ignition delay

## Subscripts

$a$  : Air  
 $b$  : Breakup

\* Corresponding Author,

**E-mail :** dohoy@umich.edu

**TEL :** +1-734-764-5263; **FAX :** +1-734-764-4256

Department of Mechanical Engineering, The University of Michigan, Ann Arbor, MI 48109-2121, USA.  
 (Manuscript **Received** September 18, 2003; **Revised** February 2, 2004)

<i>e</i>	: Equilibrium
<i>exp</i>	: Expansion stroke
<i>f</i>	: Fuel
<i>fv</i>	: Fuel vapor
<i>i</i>	: Injection
<i>l</i>	: Liquid
<i>m</i>	: Mixing controlled phase
<i>mix</i>	: Mixture
<i>n</i>	: Nozzle
<i>ox</i>	: Oxygen
<i>p</i>	: Premixed phase
<i>s</i>	: Soot emitted
<i>sf</i>	: Soot formed
<i>so</i>	: Soot oxidized
<i>z</i>	: Zone

## 1. Introduction

Design, development and optimization of a diesel engine aimed at high fuel economy and low emissions are time-intensive processes and involve a lot of experiments with expensive prototypes. As the available technical options increase, exploring the options through hardware experiments alone would not only be a very expensive and time-consuming proposition, but would also run the risk of not yielding a globally-optimized solution at the systems level. Therefore, use of the validated simulation with computational efficiency and reasonable fidelity could be an efficient methodology during the development process of globally optimized engines. Engine cycle simulation as a design optimization tool should be able to predict emissions because current challenge of diesel engine design is to reduce emissions to meet the regulations, which is more stringent than ever before. Computational efficiency and short execution time of the simulation is another critical requirement for the simulations aimed at design optimization purpose because design optimization studies require significant number of program executions to provide globally optimized solution.

Diesel engine simulation models can be classified into three categories, zero-dimensional, single-zone models, quasi-dimensional, multi-zone models and multi-dimensional models. Zero-

dimensional models (e.g., Assanis and Heywood, 1986) are not appropriate to account for exhaust emissions due to the lack of spatial information. On the other hand, multi-dimensional models, like KIVA (Amsden et al., 1985; Kim and Sung, 2001; Yeom et al., 2002) resolve the space of the cylinder on a fine grid, thus providing a formidable amount of special information. However, computational time and storage constraints still restrain these codes from routine use for design optimization purposes. As an intermediate, quasi-dimensional, multi-zone models (e.g., Im and Huh, 2000) can be effectively used to model diesel engine combustion systems.

Assanis and Heywood (1986) earlier developed a zero-dimensional thermodynamic model based engine cycle simulation, which does not have the capability of predicting emissions. The authors developed a new combustion model with a quasi-dimensional multi-zone concept (Jung and Assanis, 2001) based on their frame work of engine cycle simulation in order to add the emissions predicting capability. The quasi-dimensional multi-zone model can predict engine performance and emissions satisfactorily and is considered to be a good engine cycle simulation tool. However, computational time is increased due to emission related calculations in a number of zones compared to zero-dimensional model. Accordingly it was not practical to use the model for optimization studies which involve many design parameters. Therefore, a new concept of reduced quasi-dimensional combustion model was developed to improve the computational speed and detailed information of the reduced model is presented in this paper.

## 2. Reduced Quasi-Dimensional Combustion Model

In this section, the concept of the original quasi-dimensional, multi-zone, DI diesel combustion model developed by the authors (Jung and Assanis, 2001) are described and the following part explains a reduced quasi-dimensional model which is newly developed to improve the computational efficiency of the original model.

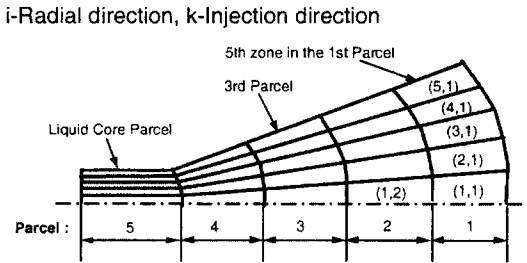


**Fig. 1** The evolution of fuel parcels and zones in the multi-zone model

Figure 1 illustrates the evolution of fuel parcels and zones in the original multi-zone model. Fuel injected into the combustion chamber according to the fuel injection schedule forms a parcel during each time step that moves in the spray axial direction. Each fuel parcel is further divided into small zones that are distributed in the radial direction. The total number of zones in the radial direction is fixed regardless of the amount of fuel injected or the time step used. However, the total number of zones in the spray direction varies depending on the injection duration and time step size.

The fuel injected into the chamber is initially assumed to form a liquid core that travels at a speed equal to the fuel injection speed until the fuel break-up time elapses. After that, the injected fuel is distributed within a spray angle that is unique to each spray parcel and varies from one time step to another depending on the conditions. The zone angle, i.e. the injection direction of each zone is determined by dividing the spray angle with the number of radial zones. Instead of solving the full momentum equation, spray penetration is traced by using empirical correlations. The velocity of each zone is calculated by temporal differentiation of the correlation for spray tip penetration. Each zone can be located relative to the injector hole by tracking the zone angle and penetration of each zone.

Following break-up, it is assumed that fuel spray atomizes to fine droplets, each with an initial diameter equal to the Sauter Mean Diameter (SMD). All calculations related to droplet evaporation are based on this SMD. It is assumed

that fuel droplets begin to evaporate after break-up occurs. Both heat and mass transfer for a single evaporating droplet are considered in order to compute instantaneous droplet temperature, rate of evaporation and droplet diameter.

The amount of entrained air is calculated based on conservation of momentum applied to each zone. The air entrainment rate depends on the physical position of each zone, with centerline zones receiving less and edged zones receiving more air.

Combustion is assumed to start individually in each zone after the lapse of the ignition delay period. The ignition delay is calculated based on zonal temperature and pressure. During the ignition delay period, some of the injected fuel is evaporated and mixed with air, forming a combustible mixture. In the early stage, combustion occurs under premixed conditions. Premixed combustion is assumed to occur until the amount of fuel evaporated at the end of the ignition delay period has been consumed. When the entire initial fuel vapor has been consumed, combustion is assumed to be controlled by diffusion of air into fuel zones.

Each zone is considered as an open system control volume and mass, energy and species equations for each zone are solved. NO and soot concentrations are also calculated for each zone based on the zonal temperature, pressure and compositions.

It was demonstrated that the quasi-dimensional multi-zone model can predict engine performance and emissions satisfactorily in the previous paper (Jung and Assanis, 2001). However, computational time was increased due to emissions modeling in a number of zones compared to zero-dimensional model. Even though the model runs much faster than the multi-dimensional model, it is not fast enough to be integrated with the high fidelity vehicle and engine system simulation as previously discussed. Therefore, it required to develop a computationally more efficient model while maintaining essential features of the original model, including the capability of predicting fuel spray evolution, ignition delay, combustion, and exhaust emissions.

As the first step of developing high speed version of quasi-dimensional multi-zone model, the physical importance of each sub-model was re-assessed and evaluated to investigate any possibility of simplifying the sub-models. Computational load of each sub-model was also considered during the development process. Then, new method of dividing and defining zones was investigated for the computational improvement.

Sub-models used in the original quasi-dimensional spray combustion model include spray penetration, air entrainment, fuel evaporation, combustion, and emissions models. Spray penetration is calculated using empirical correlations without solving time consuming momentum equations. Therefore computational load on tracing spray penetration is not significant. The amount of air entrained into each zone is calculated based on a relatively simple momentum conservation concept in conjunction with spray penetration information. Air entrainment calculation does not cause any significant computational load, either. Since the calculations of combustion rate and NO and soot emissions formation rates highly depend on the concentration of the air in the zones, it is critically important to calculate the air entrainment accurately. For these reasons, spray penetration and air entrainment are decided to be calculated for each zone defined as in the original model. (Refer to Fig. 1) As for fuel evaporation process, the equations used for the process are relatively stiff computationally because the rate of change of evaporating fuel is quite fast. Because of that, time steps for integration during the evaporation period need to be small and this causes longer computational time. The physical importance of the evaporation process in a D.I. diesel engine could be arguable. However, several discussions on this were found in the literature. According to Chiu, Shahed and Lyn (1976), under diesel operation conditions, the chamber conditions are near or above the thermodynamic critical point of fuel. Their test results show that a major portion of the spray appears in vapor form. Droplets appear only near the nozzle exit. This finding agrees with the conclusions of

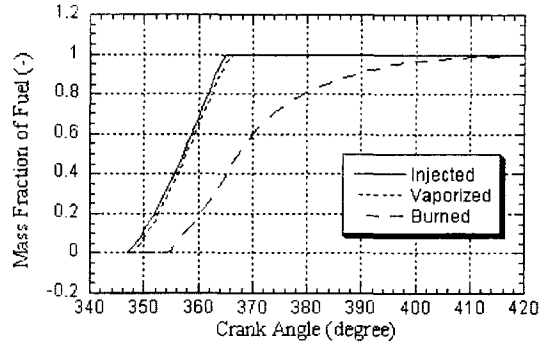


**Fig. 2** Predicted mass fractions of fuel injected, vaporized and burned at 1800 rpm, 50% load condition of 12.7 L 6 cylinder DDC 60 series engine (Jung and Assanis, 2001)

several other workers. Newman and Brzustowski (1971) showed that a liquid jet near the thermodynamic critical condition behaves as a gaseous jet. Any droplets shatter as the surface tension approaches zero near the critical point. Burt and Troth (1970) concluded from their spray evaporation experiment, as well as Waldman and co-workers (1974) from their analysis, that the evaporation of the injected fuel under diesel conditions is immediate and that a model of vaporized fuel spray is reasonable.

The simulation results from the original quasi-dimensional model also show the same observation. Figure 2 is an example of the results. It shows predicted mass fractions of fuel injected, vaporized and burned from a typical DI heavy duty diesel engine (Jung and Assanis, 2001). As shown in Fig. 2, the period of fuel evaporation, which is the interval between the accumulated mass of fuel injected and the mass of fuel vaporized, is the order of 1 degree crank angle. Therefore, it is reasonable to conclude that the evaporation of the injected fuel is fast and that a model of vaporized fuel spray is possible under normal operating conditions. Thus, fuel evaporation sub-model is eliminated in the new model.

Combustion and emissions formation sub-models are the others that cause computational inefficiency of the original model. Especially NO formation sub-model based on the extended

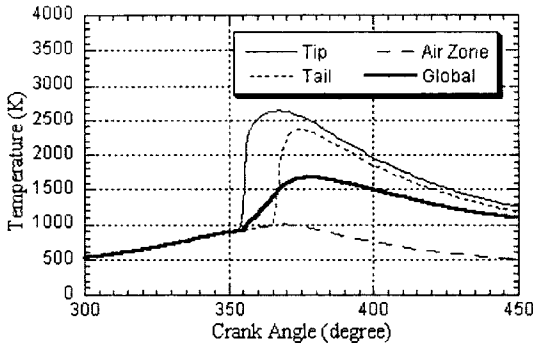


**Fig. 3** Predicted temperatures of spray tip, tail, and air zone compared with global gas temperature at 1800 rpm, 50% load (Jung and Assanis, 2001)

Zeldovich mechanism requires significant amount of computation time during the process of calculating equilibrium concentrations of 14 different species for each zone. One of the reasons to divide the fuel spray into a number of zones is to provide more accurate temperature distribution within the spray to the combustion and emissions models since they are highly sensitive to the temperature. As shown in the previous study, the temperatures of burning or burned zones, which are represented by the spray tip and tail temperatures in Fig. 3, are much higher than the global cylinder temperature. This is because the global cylinder gas temperature is the mean value of high temperature gas within the spray and low temperature ambient gas in the cylinder. This explains why zero-dimensional or single zone models are not suitable for emissions predictions. However, the temperature difference between the spray tip and tail is not significant. Based on this observation, aggregated spray zone concept is introduced to the new model to reduce the computational time caused by the combustion and emissions formation sub-models. Unlike the case of spray penetration, and air entrainment calculations, only three zones are considered for the calculation of spray combustion and emissions formation processes. The definition of zones for spray combustion and pollutant formations is illustrated in Fig. 4. The spray is divided into liquid core zone and aggregated zone and the

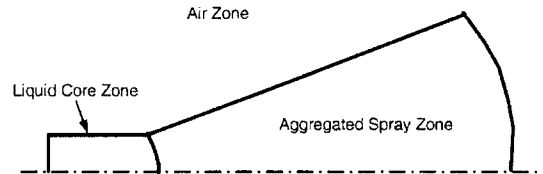


**Fig. 4** Definition of zones for spray combustion and pollutant formations

ambient air zone is distinguished from those two zones mainly due to the different level of temperatures of the zones. Conservation equations of mass and energy are applied to air zone and aggregated spray zone to calculate thermodynamic properties. NO and soot emissions are calculated for the aggregated zone based on its temperature and compositions. By defining different zones for different processes, computational time can be significantly reduced without losing the capability of predicting emissions.

### 3. Sub-Models

#### 3.1 Spray penetration

Spray penetration is calculated with empirical correlations proposed by Jung and Assanis (2001). The correlations proposed by Hiroyasu and Arai (1980) were modified to generalize their correlations so as to handle nozzles with arbitrary discharge coefficients.

a) Before breakup,  $0 < t < t_b$

$$S = C_D \left( \frac{2\Delta P}{\rho_l} \right)^{0.5} t \quad (1)$$

b) After breakup,  $t_b < t$

$$S = 2.95 \left( \frac{\Delta P}{\rho_a} \right)^{0.25} (d_n t)^{0.5} \quad (2)$$

where breakup time,  $t_b$ , is

$$t_b = 4.351 \frac{\rho_l d_n}{C_D^2 (\rho_a \Delta P)^{0.5}} \quad (3)$$

#### 3.2 Air entrainment

The air entrainment rate into a given zone is controlled by the conservation of momentum applied to the zone. It is assumed that the momentum of the zone at any instant is equal

to the momentum imparted in the zone upon nozzle exit. Since the mass of fuel and injection velocity of each zone are initially determined and the velocity of the zone can be subsequently calculated, the amount of air entrained is obtained by the momentum conservation equation. The equation for air entrainment rate can be obtained by Jung and Assanis (2001)

$$\dot{m}_a = -\frac{m_f u_i}{(dS/dt)^2} \frac{d^2 S}{dt^2} \quad (4)$$

### 3.3 Combustion

In general, ignition delay is a complicated function of mixture temperature, pressure, equivalence ratio, and fuel properties. For the purposes of diesel combustion simulations, simplified Arrhenius expression of the form (Watson et al., 1980)

$$\tau = 3.45 P^{-1.02} \exp\left(\frac{2100}{T}\right) \quad (5)$$

is used. During the ignition delay period, some of the injected fuel is evaporated and mixed with air, forming a combustible mixture. Following ignition, the first phase of combustion occurs under premixed conditions at a rate of  $RR_p$  given by the following Arrhenius type kinetic equation (Nishida and Hiroyasu, 1989).

$$RR_p = B_p \rho_{\max}^2 x_{fv} x_{ox}^5 \exp\left(-\frac{10000}{T_z}\right) V_z \quad (6)$$

Equation (6) is assumed to be valid until the amount of fuel evaporated during the ignition delay period has been consumed.

After the entire initial fuel vapor has been consumed, combustion is assumed to proceed to the mixing-controlled and late combustion phases. It is therefore proposed that the combustion rate for the mixing-controlled and late combustion phases are governed by the following expression (Jung and Assanis, 2001).

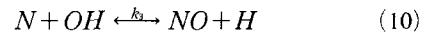
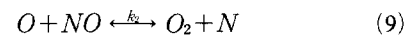
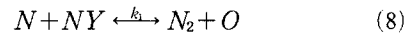
$$RR_m = B_m m_{fv} \frac{P_{ox}}{P} P^{0.25} \exp\left(-\frac{3750}{T_z}\right) \quad (7)$$

If the combustion is mixing-limited, i.e. the amount of fuel available in the zone is less than the one calculated by equation (7), only the

available fuel is burned. If the combustion is kinetically limited, the fuel is burned at the rate determined by equation (7).

### 3.4 Nitric oxide emissions

While nitric oxide (NO) and nitrogen dioxide are usually grouped together as NOx emissions, NO is predominant in diesel engines (Heywood, 1988). Therefore, only NO formation is considered in the present study. Nitric oxide forms throughout the high-temperature burned gases behind the flame through chemical reactions involving nitrogen and oxygen atoms and molecules, which do not attain chemical equilibrium. The principal reactions governing the formation of NO from molecular nitrogen and its destruction are (Lavoie et al., 1970):



where forward rate constants,  $k_1$ ,  $k_2$ , and  $k_3$  are in  $m^3/kmole/s$ :

$$k_1 = 1.6 \times 10^{10} \quad (11)$$

$$k_2 = 1.5 \times 10^6 T \exp\left(-\frac{19500}{T}\right) \quad (12)$$

$$k_3 = 4.1 \times 10^{10} \quad (13)$$

This is often called the extended Zeldovich's mechanism. Zeldovich suggested the importance of reactions (8) and (9) and Lavoie et al. (1970) added reaction (10) to the mechanism. The rate of change of NO concentration is expressed as follows (Heywood, 1988):

$$\frac{d[NO]}{dt} = \frac{2R_1\{1 - ([NO]/[NO]_e)^2\}}{1 + ([NO]/[NO]_e) R_1/(R_2 + R_3)} \quad (14)$$

where

$$R_1 = k_1 [NO]_e [N]_e \quad (15)$$

$$R_2 = k_2 [NO]_e [N]_e \quad (16)$$

$$R_3 = k_3 [NO]_e [N]_e \quad (17)$$

[ ] in Eqs. (14) to (17) denotes species concentration in kmole/m<sup>3</sup>. The NO formation in the aggregated zone can be calculated with Eq. (14).

### 3.5 Soot formation and oxidation

Soot forms in the rich unburned-fuel-containing core of the fuel sprays, within the flame region, where the fuel vapor is heated by mixing with hot burned gases. Soot then oxidizes in the flame zone when it contacts unburned oxygen. Therefore, the concentration of soot in the exhaust is governed by the formation and oxidation of soot during the engine cycle, i.e.

$$\frac{dm_s}{dt} = \frac{dm_{sf}}{dt} - \frac{dm_{so}}{dt} \quad (18)$$

The general fact that the net soot formation rate is primarily affected by pressure, temperature and equivalence ratio has been fairly well established. However, the details of the mechanism leading to soot formation are not known. Consequently, semi-empirical, two-rate equation models have been used to describe the soot dynamics. In particular, the soot formation model proposed by Hiroyasu et al. (1983) is used in many multi-zone models. The formation rate is calculated by assuming a first-order reaction of vaporized fuel,  $m_{fv}$ , as follows:

$$\frac{dm_{sf}}{dt} = A_{sf} m_{fv} P^{0.5} \exp\left(\frac{-E_{sf}}{RT}\right) \quad (19)$$

The soot oxidation is predicted by assuming a second-order reaction between soot,  $m_s$ , and oxygen.

$$\frac{dm_{so}}{dt} = A_{so} m_s \frac{P_{ox}}{P} P^{1.8} \exp\left(\frac{-E_{so}}{RT}\right) \quad (20)$$

where  $E_{sf} = 5.23 \times 10^4$  kJ/kmol and  $E_{so} = 5.86 \times 10^4$  kJ/kmol.  $A_{sf}$  and  $A_{so}$  are constants that are determined by matching the calculated soot with the measured data in the exhaust gas.

## 4. Results and Discussion

### 4.1 Model calibration

Critical sub-models, such as for the heat release and soot formation processes, contain empirical

**Table 1** Engine specifications and data availability

Engine	DDC 60	CAT 3406
Type	Multi-cylinder	Single-cylinder
Bore (mm)	130	137
Stroke (mm)	160	165
Comp. Ratio (-)	15	15
Rated Speed (rpm)	2100	2100
Rated Power (kW)	350	54

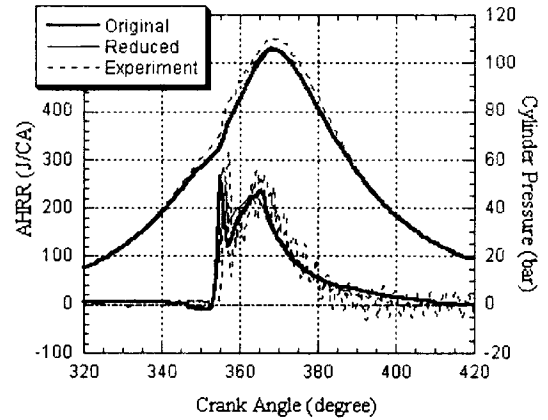


**Fig. 5** Predicted and measured cylinder pressures and apparent heat release rates

constants that need to be calibrated against experiments. The calibration constants of the heat release correlations,  $B_p$  and  $B_m$  in Eqs. (6) and (7), were calibrated with DDC 60 series 12.7 L, 6 cyl. engine data at a single operating point, which is 1800 rpm at 50% load as was done before for the original model. The engine specification is listed in Table 1.

The calibration constants in two-phase heat release correlations are adjusted to match the calculated heat release rate with experimental data.  $B_p$  and  $B_m$  were determined as  $2.0 \times 10^9$  and  $1.35 \times 10^3$ , respectively. After the calibration, the constants are remained same for the rest of the calculations. Figure 5 shows the comparison of predicted and measured cylinder pressures and apparent heat release rates. As shown in the figure, the predicted cylinder pressure and heat release rate calculated by the reduced multi-zone model are well matched with experimental data. The differences between the results from the original model and those from the reduced model

**Table 2** Operating conditions

Parameter	Value
Engine speed (rpm)	1600
Equivalence ratio	0.45
Injection timing (deg. BTDC)	5, 8, 11, 13, 15
Inlet air temperature (deg. C)	36
Inlet air pressure (kPa)	184
Exhaust back pressure (kPa)	159

are small.

The other two pre-exponential constants,  $A_{sf}$  and  $A_{so}$  in the soot formation and oxidation correlations were also calibrated with reported data in Nehmer and Reitz (1994). This work on a modern single-cylinder diesel engine was selected for soot and NO emissions model calibration and validation over a range of injection timings. The engine set-up is based on a version of the Caterpillar 3406 production engine with simulated turbocharging, and is capable of producing 54 kW at a rated speed of 2100 rpm. The engine specification is listed in Table 1. The operating conditions summarized in Table 2 were chosen to reflect common loads placed on the engine (1600 rpm and equivalence ratio of 0.45, or approximately 80% load), as well as the appropriate inlet temperature and pressure conditions.

The pre-exponential constants of soot formation and oxidation correlations were calibrated to match the soot level with measurements under the baseline operating condition (11 deg. BTDC) and kept same for the rest of the calculations. Pre-exponential constants,  $A_{sf}$  and  $A_{so}$  are 130 and 2250, respectively. The calculated soot emissions is matched to 1.014 g/bhp-hr, which is from the experimental data.

#### 4.2 Model validation

To verify the accuracy of the reduced quasi-dimensional model, performance of the DDC 60 series engine was simulated and compared with experimental data for a range of engine loads and speeds.

Figures 6 compares apparent heat release rates calculated from the predicted and measured pressure traces over a range of engine loads

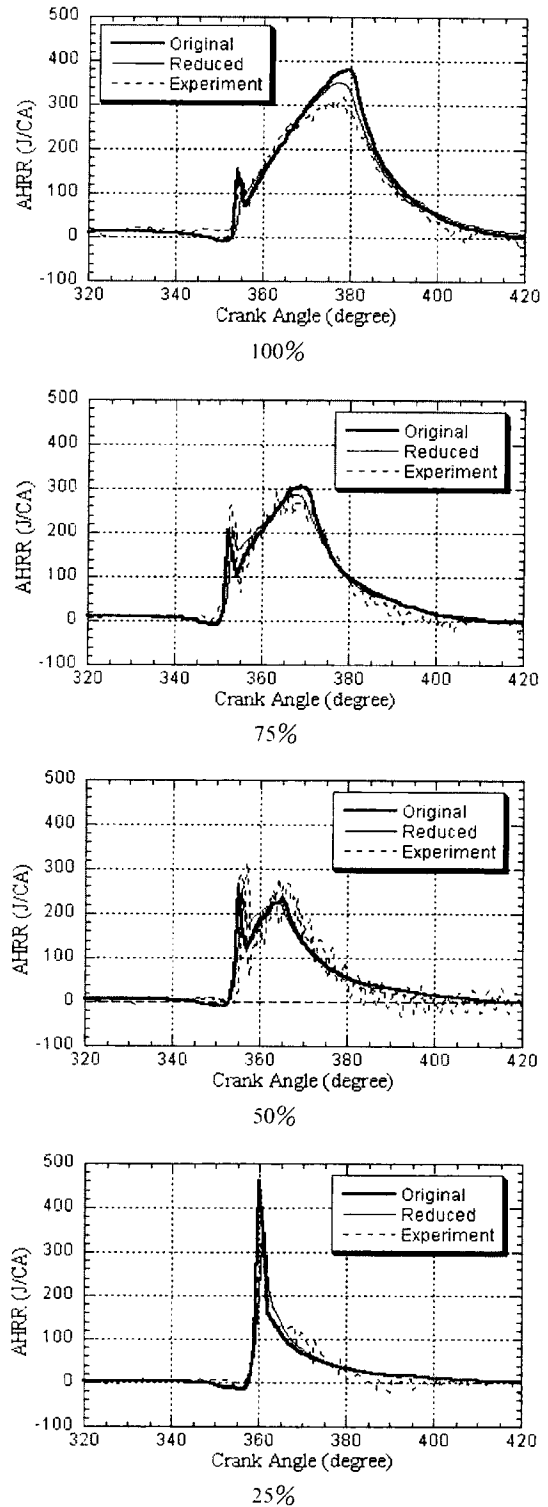


**Fig. 6** Predicted and measured apparent heat release rates over a range of loads at 1800 rpm



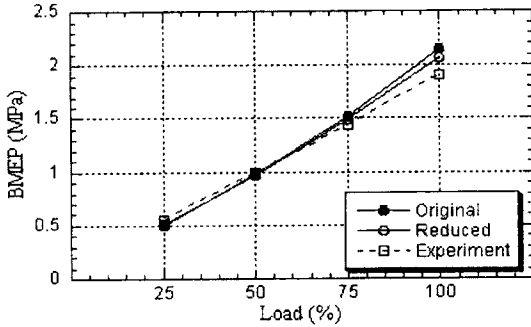


Fig. 7 Predicted and measured BMEP over a range of loads at 1800 rpm

from 25% to 100%, at a speed of 1800 rpm. Heat release rate comparisons demonstrate that the reduced multi-zone model is capable of predicting the in-cylinder phenomena over a wide range of engine loads, without losing any significant accuracy compared with the original multi-zone model.

Comparison of the predicted Brake Mean Effective Pressure (BMEP) levels with measured data at various load conditions also indicates that the reduced model predicts engine performance accurately. (Refer to Fig. 7).

The accuracy of the reduced model was explored further by comparing its predictions with experimental data acquired over a range of speeds at constant load. Engine speed was varied from 900 to 2100 rpm in increments of 300 rpm. Load was set at 50%. Figure 8 compares corresponding apparent heat release rates calculated from predicted and measured pressure traces. Overall, heat release rate comparisons show that predictions over a wide range of engine speeds are in good agreement with experimental data. Very reasonable agreement, in terms of both magnitude and trend, is also exhibited. The comparison of measured and predicted BMEP levels in Fig. 9 indicates that the reduced multi-zone model can predict engine performance reasonably well.

Additional validation of the reduced model on emissions predictions was conducted using the data from Nehmer and Reitz (1994). The pre-exponential constants of soot formation and oxidation correlations calibrated for the baseline operating condition (11 deg. BTDC) were not

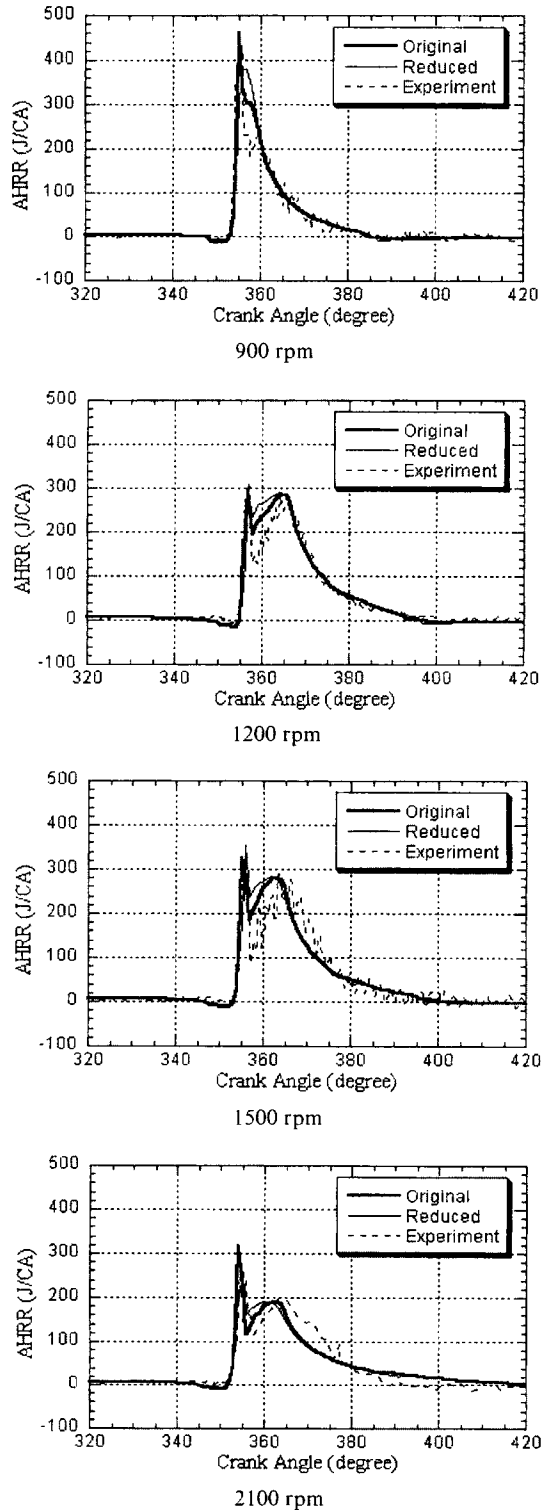


Fig. 8 Predicted and measured apparent heat release rates over a range of speeds at 50% load

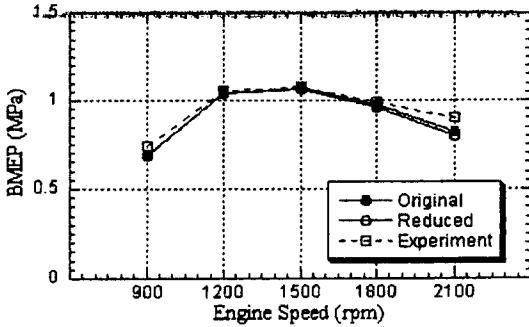


Fig. 9 Predicted and measured BMEP over a range of speeds at 50% load

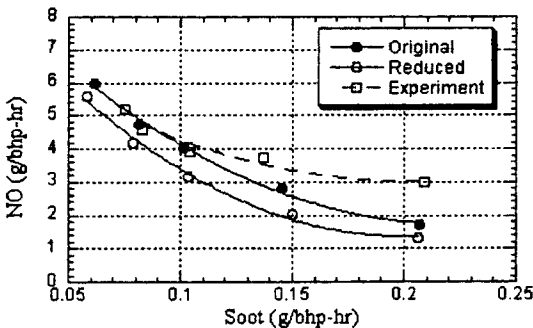


Fig. 10 Predicted and measured NO-soot trade-off curves from an injection timing sweep (5-15 CA BTDC)

changed. Beyond the baseline injection timing, predictions of emissions are compared with experimental data for injection timings of 5, 8, 13 and 15 deg. BTDC. In Fig. 10, NO-soot trade-off curves from the two alternative models are compared against measurements over a range of injection timings. While the general experimental trend can be predicted by both of the multi-zone models, the reduced model is under-predicting NO compared to the original model. This is mainly because of the effect of aggregated spray zone approach. In general, NO formation is very sensitive to temperature and NO formation rate decreases exponentially as temperature decreases. Therefore small under-prediction of the temperature of the zone could result in relatively larger errors in NO prediction. Since the temperature of the aggregated zone in the reduced model would be lower than the individual burned zones

Table 3 Comparison of normalized computational time

Model	Normalized Computational Time
Original Multi-zone Model (with emissions prediction)	217
Reduced Multi-zone Model (with emissions prediction)	1
Reduced Model (without emissions prediction)	0.6

of the original model due to the averaging effect, reduced model would under-predict NO concentration compared to the original. One possible method to resolve this problem is introducing correction factor for the temperature of the aggregated spray zone based on the ratio of burned mass and unburned mass within the aggregated zone to compensate the temperature drop due to the averaging effect.

### 4.3 Computational efficiency

The objective of this study is to develop a reduced quasi-dimensional, multi-zone, spray combustion model that is computationally efficient enough to be integrated with driveline and vehicle dynamics models while maintaining the essential features of the previously developed quasi-dimensional model. As the result of the reduction of the model with immediate fuel evaporation assumption and aggregated spray zone concept, computational time of the reduced model is significantly improved compared to the original model. To compare the computational efficiency of the reduced model accumulated computer CPU times of both reduced and original models spent for the model validation case studies are monitored. Then the normalized CPU times are compared in Table 3. The reduced model is about 200 times faster than the original model.

## 5. Conclusions

A reduced quasi-dimensional, multi-zone, di-

rect injection diesel spray combustion model has been developed based on the previously developed quasi-dimensional model and implemented in a full cycle simulation for the purpose of improving computational efficiency.

Validation of the reduced model against experimental data shows that the reduced model can predict engine performance with high fidelity and emissions in a reasonable manner and that the accuracy of the results from the reduced model is quite compatible to the original model.

The computational time of the reduced model is about 200 times faster than the original model. This improvement would make it feasible to integrate the model with driveline and vehicle dynamics models and to predict vehicle performance and emissions under dynamic transient conditions.

### Acknowledgment

The authors would like to acknowledge the technical and financial support of the Automotive Research Center (ARC) by the National Automotive Center (NAC) located within the US Army Tank-Automotive Research, Development and Engineering Center (TARDEC). The ARC is a U.S. Army Center of Excellence for Automotive Research at the University of Michigan, currently in partnership with 7 other universities nationwide.

### References

- Amsden, A. A., Ramshaw, J. D., O'Rourke, P. J., and Dukowicz, J. K., 1985, "KIVA: A Computer Program for Two- and Three-Dimensional Fluid Flow with Chemical Reactions and Fuel Sprays," *Los Alamos National Laboratory Report*, LA-10245-MS.
- Assanis, D. N. and Heywood, J. B., 1986, "Development and Use of a Computer Simulation of the Turbocompounded Diesel System for Engine Performance and Component Heat Transfer Studies," SAE paper 860329.
- Burt, R. and Troth, K. A., 1970, "Penetration and Vaporization of Diesel Fuel Sprays," Institution of Mechanical Engineers.
- Chiu, W. S., Shahed, S. M. and Lyn, W. T., 1976, "A Transient Spray Mixing Model for Diesel Combustion," SAE Paper 760128.
- Heywood, J. B., 1988, *Internal Combustion Engine Fundamentals*, McGraw-Hill Book Co.
- Hiroyasu, H., Kadota, T. and Arai, M., 1983, "Development and Use of a Spray Combustion Modeling to Predict Diesel Engine Efficiency and Pollutant Emissions (Part 1 Combustion Modeling)," *Bulletin of the JSME*, Vol. 26, No. 214, pp. 569~575.
- Hyroyasu, H. and Arai, M., 1980, "Fuel Spray Penetration and Spray Angle of Diesel Engines," *Trans. of JSAE*, Vol. 21, pp. 5~11.
- Im, Y. H. and Huh, K. Y., 2000, "Phenomenological Combustion Modeling of a Direct Injection Diesel Engine with In-Cylinder Flow Effects," *KSME International Journal*, Vol. 14, No. 5, pp. 569~581.
- Jung, D. and Assanis, D. N., 2001, "Multi-Zone DI Diesel Spray Combustion Model for Cycle Simulation Studies of Engine Performance and Emissions," *SAE Trans.: Journal of Engines*, Vol. 110, No. 3, pp. 1510~1532.
- Kim, H. S. and Sung, N. W., 2001, "Multi-dimensional Engine Modeling: NO and Soot Emissions in a Diesel Engine with Exhaust Gas Recirculation," *KSME International Journal*, Vol. 15, No. 8, pp. 1196~1204.
- Lavoie, G. A., Heywood, J. B. and Keck, J. C., 1970, "Experimental and Theoretical Investigation of Nitric Oxide Formation in Internal Combustion Engines," *Combust. Sci. Technol.*, Vol. 1, pp. 313~326.
- Nehmer, D. A. and Reitz, R. D., 1994, "Measurement of the Effect of Injection Rate and Split Injections on Diesel Engine Soot and NOx Emissions," SAE Paper 940668.
- Newman, J. A. and Brzustowski, T. A., 1971, "Behavior of a Liquid Jet Near the Thermodynamic Critical Region," *AIAA journal*, Vol. 9, No. 8.
- Nishida, K. and Hiroyasu, H., 1989, "Simplified Three-Dimensional Modeling of Mixture Formation and Combustion in a D.I. Diesel Engine," SAE Paper 890269.

- Waldman, C. H., Kau, C. J. and Wilson, R. P., Jr., 1974, "Prediction of Transient Temperature Fields within a Vaporizing/Burning Fuel Droplet under High Ambient Pressure," Western States Section, Combustion Institute, California State University at Northridge.
- Watson, N., Pilley, A. D. and Marzouk, M. A., 1980, "Combustion Correlation for Diesel Engine Simulation," SAE Paper 800029.
- Yeom, J. K., Lee, M. J., Chung, S. S., Ha, J. Y., Senda, J. and Fujimoto, H., 2002, "A Proposal for Diesel Spray Model Using a TAB Breakup Model and Discrete Vortex Method," *KSME International Journal*, Vol. 16, No. 4, pp. 532~548.